



**HAL**  
open science

## Synthesis of a new diarylhydrazone derivative and an evaluation of its in vitro biofilm inhibition and quorum sensing disruption along with a molecular docking study

Sameh Boudiba, Alfred Ngenge Tamfu, Karima Hanini, Ilhem Selatnia, Louiza Boudiba, Ibtissam Saouli, Paul Mosset, Ozgur Ceylan, Daniel Ayuk Mbi Egbe, Assia Sid, et al.

### ► To cite this version:

Sameh Boudiba, Alfred Ngenge Tamfu, Karima Hanini, Ilhem Selatnia, Louiza Boudiba, et al.. Synthesis of a new diarylhydrazone derivative and an evaluation of its in vitro biofilm inhibition and quorum sensing disruption along with a molecular docking study. *Journal of Chemical Research*, 2023, 47 (4), 10.1177/17475198231184603 . hal-04192805

**HAL Id: hal-04192805**

**<https://hal.science/hal-04192805>**

Submitted on 19 Feb 2024

**HAL** is a multi-disciplinary open access archive for the deposit and dissemination of scientific research documents, whether they are published or not. The documents may come from teaching and research institutions in France or abroad, or from public or private research centers.

L'archive ouverte pluridisciplinaire **HAL**, est destinée au dépôt et à la diffusion de documents scientifiques de niveau recherche, publiés ou non, émanant des établissements d'enseignement et de recherche français ou étrangers, des laboratoires publics ou privés.



Distributed under a Creative Commons Attribution - NonCommercial 4.0 International License

# Synthesis of a new diarylhydrazone derivative and an evaluation of its in vitro biofilm inhibition and quorum sensing disruption along with a molecular docking study

Journal of Chemical Research

May-June 1–12

© The Author(s) 2023


Article reuse guidelines:

sagepub.com/journals-permissions

DOI: 10.1177/17475198231184603

journals.sagepub.com/home/chl



Sameh Boudiba<sup>1</sup>, Alfred Ngenge Tamfu<sup>2,3,4</sup> , Karima Hanini<sup>5</sup>,  
Ilhem Selatnia<sup>6</sup>, Louiza Boudiba<sup>1</sup>, Ibtissam Saouli<sup>1,7</sup>, Paul Mosset<sup>8</sup>,  
Ozgur Ceylan<sup>3</sup>, Daniel Ayuk Mbi Egbe<sup>9,10</sup>, Assia Sid<sup>5</sup> and  
Rodica Mihaela Dinica<sup>4</sup>

## Abstract

Molecules that target quorum sensing and biofilm inhibition are useful antimicrobials. In this regard, a new diarylhydrazone was synthesized and characterized using infrared, high-resolution mass spectrometry and nuclear magnetic resonance experiments as *N*-[(*E*)-4-bromo-2,5-diheptyloxybenzylideneamino]-2,4-dinitroaniline (BHBANA). Minimal inhibitory concentrations (MICs) vary from 0.625 to 2.5 mg mL<sup>-1</sup>. This compound was screened in vitro for its inhibition of quorum sensing-mediated violacein production by *Chromobacterium violaceum* CV12472 at MIC and sub-MIC and showed percentage inhibition varying from 100% at MIC to 5.7% ± 0.2% at MIC/32. Against *Chromobacterium violaceum* CV026, BHBANA exhibited anti-quorum-sensing zone diameters of 10.5 ± 0.3 mm and 7.0 ± 0.1 mm at MIC and MIC/2, respectively. BHBANA shows concentration-dependent inhibition of swarming motility on flagellated *Pseudomonas aeruginosa* PAO1 with the highest % inhibition of 28.30% ± 0.50% µg mL<sup>-1</sup> at MIC. The product inhibits biofilm formation, with the best biofilm inhibition being observed against *Staphylococcus aureus* varying from 72.24% ± 0.86% (MIC) to 09.82% ± 0.10% (MIC/8). Molecular docking studies carried out utilizing the Schrodinger software identified interactions between BHBANA and different receptor compartments of *Chromobacterium violaceum*, which can block pathogenic gene expression. The results suggest the potential of BHBANA in reducing microbial virulence.

## Keywords

anti-biofilm, hydrazone, molecular docking, *N*-[(*E*)-4-bromo-2,5-diheptyloxybenzylideneamino]-2,4-dinitroaniline, quorum sensing, swarming motility

Date received: 8 March 2023; accepted: 11 June 2023

<sup>1</sup>Laboratory of Applied Chemistry and Renewable Energies (LACRE), Echahid Cheikh Larbi Tebessi University, Tebessa, Algeria

<sup>2</sup>Department of Chemical Engineering, School of Chemical Engineering and Mineral Industries, University of Ngaoundere, Ngaoundere, Cameroon

<sup>3</sup>Food Quality Control and Analysis Program, Ula Ali Kocman Vocational School, Mugla Sitki Kocman University, Mugla, Turkey

<sup>4</sup>Department of Chemistry, Physics and Environment, Faculty of Sciences and Environment, Dunarea de Jos University, Galati, Romania

<sup>5</sup>Laboratory of Bioactive Molecules and Applications (LBMA), Echahid Cheikh Larbi Tebessi University, Tebessa, Algeria

<sup>6</sup>Laboratory of Analytical Sciences, Materials and Environmental (LASME), Larbi Ben M'Hidi University, Oum El Bouaghi, Algeria

<sup>7</sup>Department of Chemistry, Faculty of Sciences, Badji Mokhtar University, Annaba, Algeria

<sup>8</sup>CNRS, ISCR (Institut des Sciences Chimiques de Rennes), University of Rennes, Rennes, France

<sup>9</sup>Department of Chemistry, Material Science, Innovation and Modelling Research Focus Area, North-West University, Mmabatho, South Africa

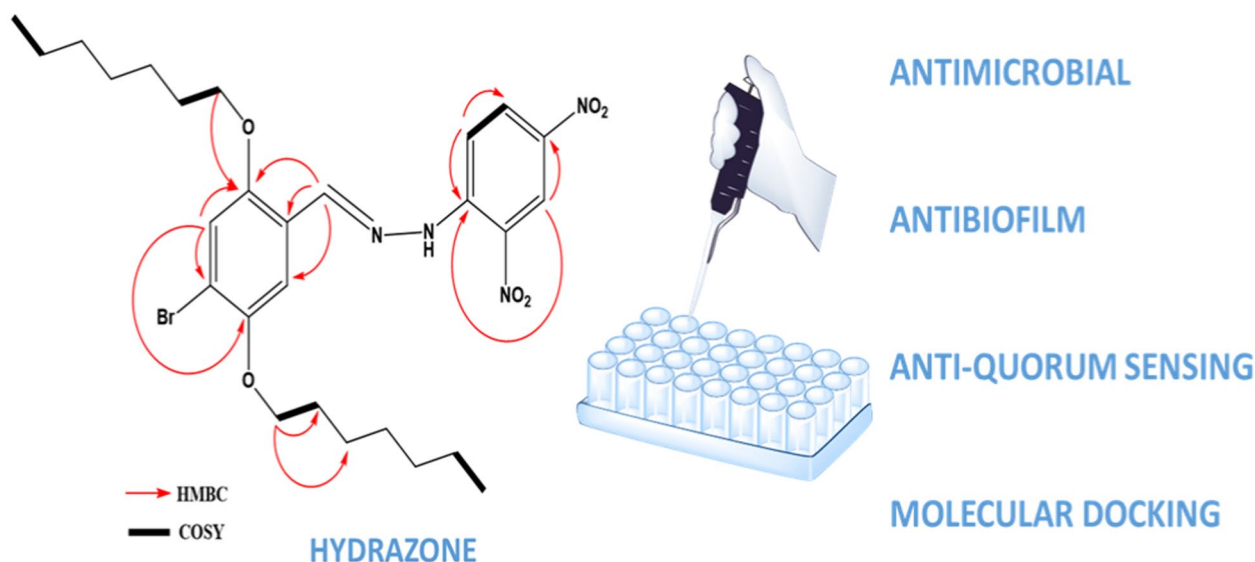
<sup>10</sup>College of Science and Technology, University of Rwanda, Kigali, Rwanda

## Corresponding author:

Alfred Ngenge Tamfu, Department of Chemical Engineering, School of Chemical Engineering and Mineral Industries, University of Ngaoundere, 454 Ngaoundere, Cameroon.

Email: macntamfu@yahoo.co.uk





## Introduction

Aryl hydrazones represent an important class of compounds for heterocyclic synthesis such as indoles and pyrazoles.<sup>1,2</sup> These molecules have several applications in biology, organic/inorganic, and analytical chemistry<sup>3,4</sup> and can act as antidepressants, anti-inflammatory, antimicrobial, antimalarial, antitumor, antioxidant, and antifungal agents.<sup>4–7</sup> Drugs such as nitrofurazone, furazolidone, and nitrofurantoin bear either hydrazide or hydrazone functions and compounds of this nature are known to possess various biological activities.<sup>8</sup> Hydrazones are therefore attractive as synthetic compounds with biological activities, and some hydrazone-based drugs such as dihydralazine, mitoguanzone, nifuroxazide, and ferimzone show clear evidence of bioactive relevance.<sup>9</sup> The structures of the hydrazone-based drugs mentioned here are given in Figure 1.

Resistance to antibiotics by pathogenic bacteria occurs when bacteria acquire the ability to overcome the effects of antibiotics that were used previously to inhibit them.<sup>10,11</sup> Antimicrobial resistance is an emerging worldwide health challenge, causing morbidities and mortalities even in hospital settings. Despite the development of conventional antimicrobials as solutions, there is a multidrug-resistant pattern in Gram-positive and Gram-negative bacteria, as well as in fungi, resulting in difficult-to-treat or even untreatable infections.<sup>10,12–14</sup> Millions of people suffer from microbial infections, some of which are caused by resistant strains, accounting for millions of deaths worldwide each year.<sup>15</sup> Bacterial biofilms are responsible for approximately 80% of severe and recurrent microbial infections in humans, and microbial cells living within biofilms maybe 10–1000 times more resistant to antibiotics than their planktonic counterparts.<sup>16</sup> Microbial pathogens can evolve and develop resistance, usually aided by quorum sensing (QS)-mediated virulence factors and biofilm formation, and this requires a multidisciplinary approach involving antimicrobial molecules of synthetic and natural origin that can act on the pathogens by various

mechanisms involving biofilms and QS.<sup>11,17,18</sup> Bacterial biofilms are aggregates of bacterial cells attached to a surface and coated with a polymeric layer.<sup>19–21</sup> They protect bacteria and allow them to survive in harsh environmental conditions.<sup>22,23</sup> They can resist immune response of the host and are much more resistant to antibiotics and disinfectants.<sup>24,25</sup> Bacteria in the biofilm are less sensitive to antibiotics and can be very resistant because of the polymeric layer, which forms a barrier, reducing or preventing the diffusion of antimicrobials.<sup>26,27</sup> The dissemination of antibiotic resistance is usually accompanied by genetic changes including genetic mutations, genetic transfer of resistance genes through plasmids, and mutations of target genes.<sup>28</sup> There are different strategies for inhibiting biofilm formation, such as inhibition of formation of the polymeric layer or its degradation, prevention of the initial microorganism adhesion, prevention of microbial growth, or the interruption of communication between bacterial cells (quorum sensing).<sup>24,29–31</sup> The search for more effective and safer antibiotic alternatives, whether herbal or synthetic, as well as new therapeutic and nonpathogenic agents that might act as nontoxic inhibitors of QS, is increasing.<sup>31–35</sup> Therefore, there is an urgent need to develop new therapies that can treat bacterial infections and overcome the emergence of drug-resistant strains and disrupt bacterial cell-to-cell communication, known as quorum sensing, and eliminate biofilm formation.<sup>36</sup>

This study presents the synthesis and characterization of a new diaryldiazene derivative and the evaluation of its effects on microbial biofilms and quorum sensing. To understand, determine, and visualize the most likely interaction of the hydrazone with the protein as a QS inhibitor and the *Chromobacterium violaceum* receptor protein, molecular docking studies have been carried out. To this end, the binding affinities, orientation, and binding modes of the docked ligands at the protein receptor active site are predicted using the docking score and hydrogen bonds made with the amino acids forming the target protein.<sup>27–38</sup>

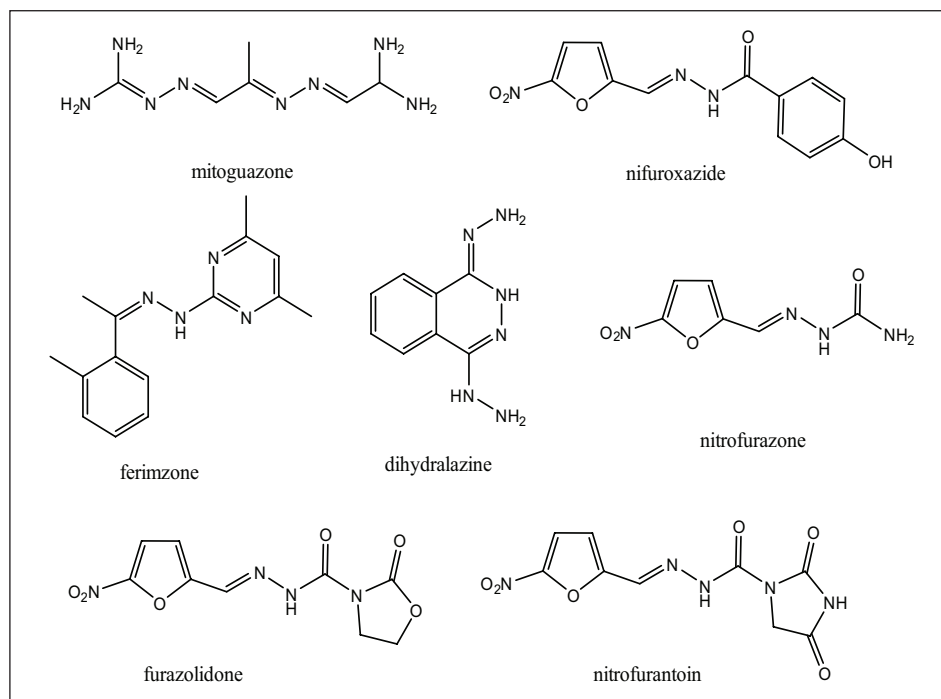


**Figure 1.** Examples of hydrazone-based drugs.

## Results and discussion

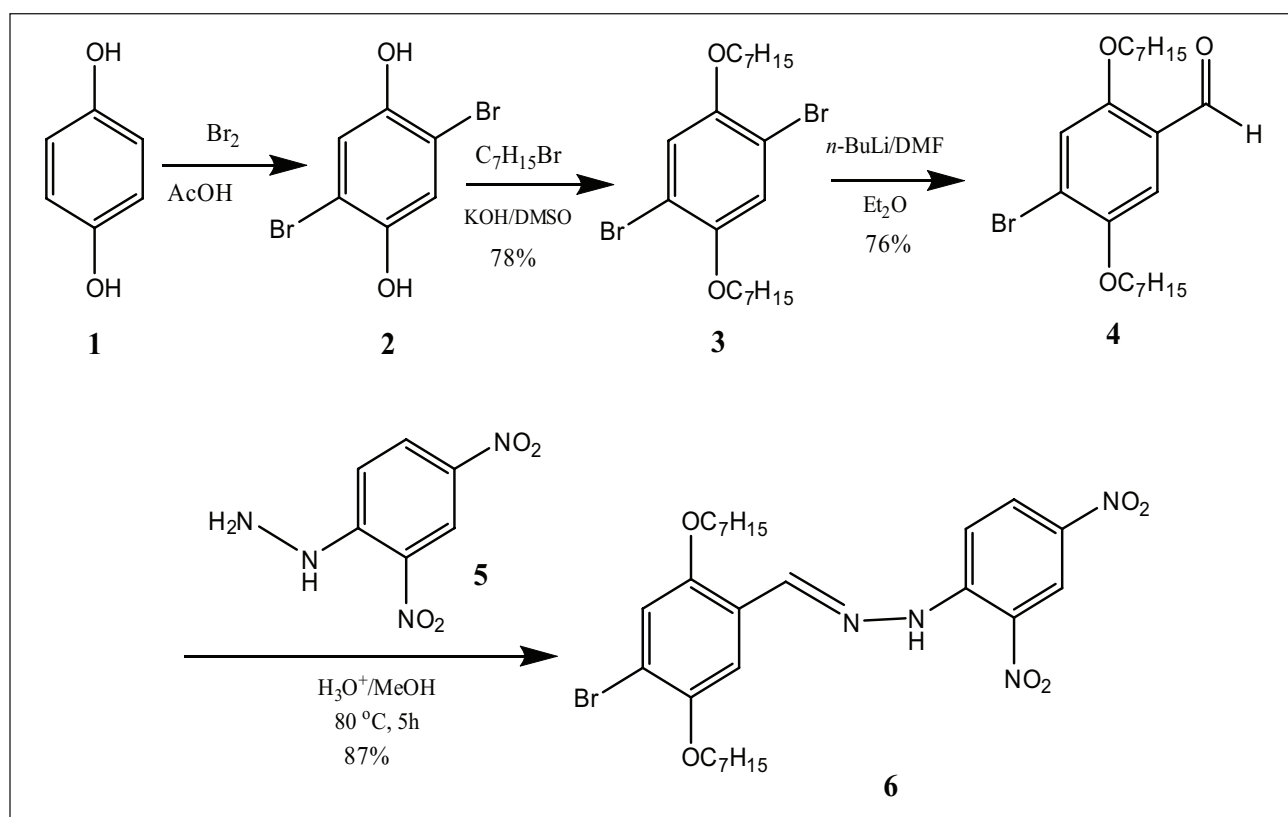
### Chemical synthesis and characterization

The new diarylhydrazone **6** was successfully synthesized in good yields from 2,4-dinitrophenylhydrazine **5** and an aromatic aldehyde **4** according to literature.<sup>39–42</sup> The reaction pathway is shown on Scheme 1 and the spectral data HRMS, IR, <sup>1</sup>H NMR, <sup>13</sup>C NMR, and 2D NMR are used for the structural elucidation. All spectra are provided in the Supporting Information.

### Violacein inhibition and anti-quorum sensing activity of BHBANA

The molecule responsible for a pigment called violacein is a derivative of an indole that results from the condensation of two molecules of tryptophan, and it has numerous biological activities.<sup>43</sup> *C. violaceum*, while growing, produces a violet coloration through a quorum sensing-mediated process, and violacein plays an antioxidant role, protecting the bacterial membrane from oxidative damage.<sup>44</sup> BHBANA (**6**) exhibits a minimal inhibitory concentration (MIC) value of 1.25 mg mL<sup>-1</sup> against *C. violaceum* CV12472, as shown in Table 1. Before the evaluation of violacein inhibition on *C. violaceum* CV12472, the MIC value of compound **6** was determined so that the violacein inhibition could be evaluated at concentrations lower than the MIC value. This is to exert selective pressure on the microbe at low concentration, allowing it to display quorum sensing processes. Compound **6** was able to inhibit violacein production at 100% at the MIC concentration, and this inhibition was reduced in a concentration-dependent manner to 5.7% ± 0.2% at MIC/32. It had a MIC value of 0.625 mg mL<sup>-1</sup> toward *C. violaceum* CV026, and its effect

on quorum sensing through signal reception from an external AHL (acyl-homoserine lactone) was evaluated at MIC and sub-MIC concentrations. Compound **6** showed quorum sensing inhibition zones of 10.5 ± 0.3 mm at MIC and 07.0 ± 0.1 mm at MIC/2. Violacein is a secondary metabolite that is produced by bacteria as a signal molecule that protects them from external hazards and environmental stress and also functions as an antibiotic against other microbes.<sup>45,46</sup> The ability of the compound to inhibit violacein production, which is a signal molecule, indicates the potential for quorum sensing inhibition through the inhibition of signal molecule production. The use of a violacein production strain in this assay is suitable and reliable since violacein is easily measurable and quantifiable, and it is an important marker trait that permits the bacterium to be used in quorum sensing research.<sup>47</sup> The biomarker strain *C. violaceum* CV026 does not produce violacein while growing unless an AHL is supplied to it externally, and therefore, if it fails to produce violacein after the supply of AHL, then it is suggested that the bacterial cells do not receive the AHL signal molecule. The quorum sensing inhibition zones correspond to a cream-colored or brown halo or circle around the wells and are measured in millimeters.<sup>31,33,44</sup> Bacterial cells failed to receive signal molecules representing the QS inhibition zone within this area. Quorum sensing involves the process by which bacteria regulate virulence factors and genes through a cell-to-cell communication network aided by the production, diffusion, and reception of produced signal molecules and auto-inducers.<sup>48–50</sup> QS is involved in the production of biofilms and the regulation of swarming movements in bacteria, and it can contribute to the development of resistance to antibiotics. Inhibition of QS is therefore very beneficial. Bacterial virulence and the establishment of biofilms are among the key processes that are mediated



**Scheme 1.** Synthesis of BHBANA (**6**).

**Table 1.** Quorum sensing inhibitory effects of BHBANA.

MIC (mgmL <sup>-1</sup> )	MIC	MIC/2	MIC/4	MIC/8	MIC/16	MIC/32
Violacein inhibition (%) against <i>C. violaceum</i> CV12472						
1.25	100 ± 0.0	85.9 ± 1.5	48.6 ± 1.0	29.5 ± 1.3	17.8 ± 0.7	5.7 ± 0.2
QS inhibition zones (diameter in mm) against <i>C. violaceum</i> CV026						
0.625	10.5 ± 0.3	7.0 ± 0.1	–	–	NT	NT
Swarming motility inhibition against <i>P. aeruginosa</i> PA01						
2.50	45.7 ± 1.1	27.5 ± 0.6	14.4 ± 0.5	NT	NT	NT

BHBANA: *N*-[(*E*)-4-bromo-2,5-diheptyloxybenzylideneamino]-2,4-dinitroaniline; MIC: minimal inhibitory concentration; QS: quorum sensing; –: no inhibition; NT: not tested.

by QS, and therefore, inhibiting QS is a suitable solution to mitigating the rise in biofouling, surface attacks, and microbial resistance.<sup>51</sup>

### Antimicrobial activity of BHBANA

The antimicrobial activity of BHBANA (**6**) was evaluated against a range of human pathogenic microbes. The test organisms consisted of three Gram-positive bacteria, two Gram-negative bacteria, and two fungal yeasts, and the concentration at which no visible microbial growth was observed is recorded as the MIC value (Table 2). For Gram-positive bacteria, the MIC values were 1.25 and 0.625 mgmL<sup>-1</sup> for *Staphylococcus aureus* and *Enterococcus faecalis*, respectively. For Gram-negative bacteria, the MIC values were 2.5 mgmL<sup>-1</sup> for both *Escherichia coli* and

*Pseudomonas aeruginosa*. The two yeasts, *Candida albicans* and *Candida tropicalis*, had the same susceptibility to the test compound, with MIC values of 0.625 mgmL<sup>-1</sup>. Therefore, compound **6** demonstrates its best antimicrobial activity against *E. faecalis*, *C. albicans*, and *C. tropicalis* and inferior antimicrobial activity against the *S. aureus*, *E. coli*, and *P. aeruginosa*. BHBANA shows potential antimicrobial activity against a range of microbes and represents a potential starting material or scaffold for antibiotic drug development. Since antibiotics usually fall out of use due to the emergence of resistance developed by pathogens toward them, it is necessary to continuously furnish new antimicrobial substances from natural and synthetic sources to provide different forms of interaction against the pathogens and to wipe them out. The rising public health problem caused by antibiotic resistance and the emergence of novel

**Table 2.** Antimicrobial and anti-biofilm activities of BHBANA.

Microorganism	Antimicrobial activity MIC (mg mL <sup>-1</sup> )	Biofilm inhibition (%)	
<i>S. aureus</i>	1.25	MIC	72.24 ± 0.86
		MIC/2	46.27 ± 0.42
		MIC/4	24.30 ± 0.18
		MIC/8	9.82 ± 0.10
<i>E. faecalis</i>	0.625	MIC	49.55 ± 0.67
		MIC/2	23.41 ± 0.35
		MIC/4	15.69 ± 0.21
<i>E. coli</i>	2.50	MIC	10.25 ± 0.16
		MIC/2	3.2 ± 0.04
		MIC/4	–
<i>P. aeruginosa</i>	2.50	MIC	28.30 ± 0.50
		MIC/2	12.50 ± 0.14
		MIC/4	–
<i>C. albicans</i>	0.625	MIC	25.83 ± 0.84
		MIC/2	10.26 ± 0.15
		MIC/4	–
<i>C. tropicalis</i>	0.625	MIC	40.15 ± 1.20
		MIC/2	23.90 ± 0.43
		MIC/4	08.73 ± 0.26
		MIC/8	–

BHBANA: *N*-[(*E*)-4-bromo-2,5-diheptyloxybenzylideneamino]-2,4-dinitroaniline; MIC: minimal inhibitory concentration; –: no inhibition.

bacterial pathogen strains necessitate an influx of new antimicrobial substances from natural products and by chemical synthesis to ameliorate infection treatment with greater efficacy.<sup>52</sup> Chemically synthesized antimicrobials have the added advantage of being able to modify their structures to improve their activity and they can be industrially synthesized and commercialized to meet the demands of the large global population. The search for antimicrobial substances is long-standing and includes natural, semi-synthetic, and synthetic compounds acting as antibacterial agents against specific pathogens. It originated from the discovery of penicillin and fusidic acid and extends to the latest contemporary approaches, which evaluate the antimicrobial effects of compounds on antibiotic resistance and the virulence factors of pathogenic bacteria.<sup>53</sup>

### Anti-biofilm activity of BHBANA

Most pathogens within the host or in the environment are capable of undergoing an extracellular encapsulation, making them protected from and resistant to antibiotics, and their infections become chronic, persistent, and difficult to treat. Therefore, the design of new antibiotics capable of targeting and disrupting biofilms and also targeting all stages of biofilm formation within the drug discovery process is a useful strategy.<sup>54</sup> Compound **6** exhibited the ability to inhibit microbial biofilms in a concentration-dependent manner, as shown in Table 2. With the Gram-positive bacteria *S. aureus*, the biofilm inhibition varied from 72.24% ± 0.86% (MIC) to 9.82% ± 0.1% (MIC/8), while against

*E. faecalis*, anti-biofilm activity varied from 49.55% ± 0.67% (MIC) to 15.69% ± 0.21% (MIC/4), and no inhibition was observed at MIC/8. Against the Gram-negative bacteria, anti-biofilm activity was observed with *E. coli* at MIC 10.25% ± 0.16% and at MIC/2 3.2% ± 0.04% as well as with *P. aeruginosa* at MIC 28.30% ± 0.50% and MIC/2 12.5% ± 0.14%. No inhibition of biofilm formation was observed for the Gram-negative bacteria below MIC/4. For the two yeast cells, biofilm inhibitions ranged from 25.83% ± 0.84% (MIC) to 10.26% ± 0.15% (MIC/2) against *C. albicans* and from 40.15% ± 1.2% (MIC) to 8.73% ± 0.26% (MIC/4) against *C. tropicalis*. Overall, the Gram-positive bacteria biofilms were the most susceptible to BHBANA. Biofilms can be established on biotic and abiotic surfaces, especially on high-touch surfaces where the contamination risk is high, and therefore, synthesized antibiotic substances like BHBANA can find applications as an encapsulated material in surface coatings on which it can help to reduce biofouling and biofilm establishment.<sup>55</sup> Biofilms represent a severe danger in medical devices as implants result in biofilm-based nosocomial infections and affect implants in patients such as prosthetic catheters, heart valves, cardiac pacemakers, dental implants, prostheses, and contact lenses.<sup>56</sup> Biofilm formation is a QS-mediated process, and it was observed above that compound **6** could inhibit QS in pathogenic bacteria. However, apart from QS inhibitors, other anti-biofilm agents act as adhesion inhibitors, efflux pump inhibitors, extracellular polymeric substance synthesis inhibitors, and cyclic diguanylate inhibitors.<sup>57</sup>

### Swarming motility inhibition in *P. aeruginosa* PA01 by BHBANA

The early stages of biofilm establishment and the dispersion of cells from biofilms consist of bacterial cells moving toward the surfaces and then colonizing the surfaces through different movements or motilities such as swimming, swarming, and twitching.<sup>58</sup> Therefore, the inhibition of swarming motility could reduce the incidence of biofilm formation and surface colonization by bacteria and prevent contamination. The ability of compound **6** to reduce swarming movements in flagellated bacteria (*P. aeruginosa* PA01) was determined at three concentrations, MIC, MIC/2, and MIC/4, and concentration-dependent variation was observed (Table 1). The inhibition of swarming motility by BHBANA was 45.7% ± 1.1% at MIC value, 27.5% ± 0.6% at MIC/2, and 14.4% ± 0.5% at MIC/4. Swarming is a surface-associated movement and behavior that helps in the colonization and rapid spread of bacterial communities, and in flagellated bacteria such as *P. aeruginosa*, swarming depends on functional flagella and is associated with the aid of biosurfactant production.<sup>58,59</sup> The opportunistic pathogen, *P. aeruginosa*, can cause various infections in plants and animals, including humans, because of the production of various virulence factors such as QS-mediated swarming, swimming, and twitching motilities that facilitate the infection process.<sup>60,61</sup> The ability of BHBANA to inhibit swarming motility, which is a QS-mediated movement and an important step in biofilm formation and biofilm dispersion, is a good indication that compound **6** has great potential as a novel class of antibiotic that can inhibit quorum sensing, the multiple steps involved in biofilm formation and the development of resistance.

The positive effects of compound **6** on swarming motility, violacein production, and QS inhibition at low concentrations are desirable since this can help to reduce the virulence factors of the pathogens during infections.<sup>62</sup> When antibiotics are administered at sub-inhibitory doses, that is, concentrations lower than the MIC, the bacteria can easily develop resistance to this antibiotic with time by developing biofilms. Therefore, new antibiotics that are capable of inhibiting biofilms at MIC and sub-MIC concentrations without necessarily killing the bacteria are new desired leads for antimicrobial agents. This is the major reason why biofilm and anti-quorum sensing studies are performed at MIC and sub-MIC concentrations to better understand their effects on virulence factors and the elimination of microbial resistance.

### Molecular docking analysis

Molecular docking contributes to improve the understanding of the interaction between the active sites of CviR and the BHBANA. This study targeted *C. violaceum* ATCC 12472 using the newly synthesized BHBANA, and FAD [(2*R*, 3*S*, 4*R*, 5*R*)-5-(6-aminopurin-9-yl)-3,4-dihydroxyoxolan-2-yl]methoxy-hydroxyphosphoryl], used as a reference ligand. These interactions are illustrated in Figures 2 and 3 and their binding affinities toward the target protein are presented as distance and bonding parameters of BHBANA and FAD toward the active sites of CviR in Table 3.

As can be seen in Figure 2, the active sites of the target proteins were the Lys33, Leu40, Tyr192, Arg249, Arg97, Thr145, Arg105, and Phe251 amino acid residues, where the interactions with BHBANA were concentrated. The 3D orientation (Figure 3) reveals the hydrophobic sites and hydrogen bonds of both the BHBANA and FAD molecules. Similarities between the results reported in the literature for the FAD<sup>63</sup> and those for BHBANA are observed as strong hydrophobic interactions around Leu40, Val44, Val141, Tyr163, Tyr192, Ile202, Phe251, and Phe276. These interactions are attributed to the presence of the heptyl side chain in the BHBANA backbone. The results in Table 3 further show that the distances, categories, and types of hydrogen bonding for the two molecules under study (FAD and BHBANA) are convergent, if not similar. It should be noted that BHBANA has slightly smaller distances than FAD, which gives the protein–ligand complex it forms higher stability and robustness. In addition, hydrogen bonding and salt bridge interactions were detected in the active sites. It should be recalled that the interaction through hydrogen bonding is significant in inducing QS activity in the CviR protein.<sup>64</sup> From the previous docking visualization, the newly synthesized molecule adopts a very similar orientation in the active site to that revealed with FAD, which could play an important role in overcoming the QS system in *C. violaceum* (CV12472). It is important to point out that the results from the Swiss-ADME web server show that the tested BHBANA has a molecular weight (MW) of 593.51 g mol<sup>-1</sup>, which is lower than that of the reference molecule (FAD) (785.55 g mol<sup>-1</sup>), which induces better absorption. For this reason, it can be administered orally or parenterally, compared with FAD, which is only prescribed in injectable form. Furthermore, and because LogP is a crucial pharmacokinetic characteristic, the novel molecule has a LogP (iLOGP) value of 5.5, which results in a better dispersion in lipid and aqueous media than FAD, which has a LogP value of 0.5. Hence, even if the free energy of binding ( $\Delta G$ ) of BHBANA is higher (-7.697 kcal mol<sup>-1</sup>) compared to a  $\Delta G$  value of -15.098 kcal mol<sup>-1</sup> for FAD. This may be a result of the fact that the structure of FAD is more complex than that of BHBANA (**6**), making it to establish more hydrogen bond interactions with the amino acids in the proteins. Illustratively, six hydrogen bonds are observed with FAD (Lys33 with a hydroxyl group, Ash269 and Ala11 with the oxygen of the phosphate ion PO<sub>4</sub><sup>-</sup>, Thr262 with oxygen, and Val45 with oxygen atom, hydrogen atom with Val 45), while only two are observed with BHBANA (Ala11 with the oxygen of the nitro-group and Arg249 with the heptyloxyl oxygen). Considering both parameters cited above (MW and LogP), BHBANA is still advantageous for further exploitation and may pave the way to design potent compounds with significant QS system inhibition potential toward *C. violaceum* (CV12472).

### Conclusion

In this work, a new diarylhydrazone derivative was successfully synthesized in a good yield of 87%, and its structure was characterized using mass spectrometry and extensive NMR experiments. The newly synthesized hydrazine compound, BHBANA (**6**), was evaluated for its effect on

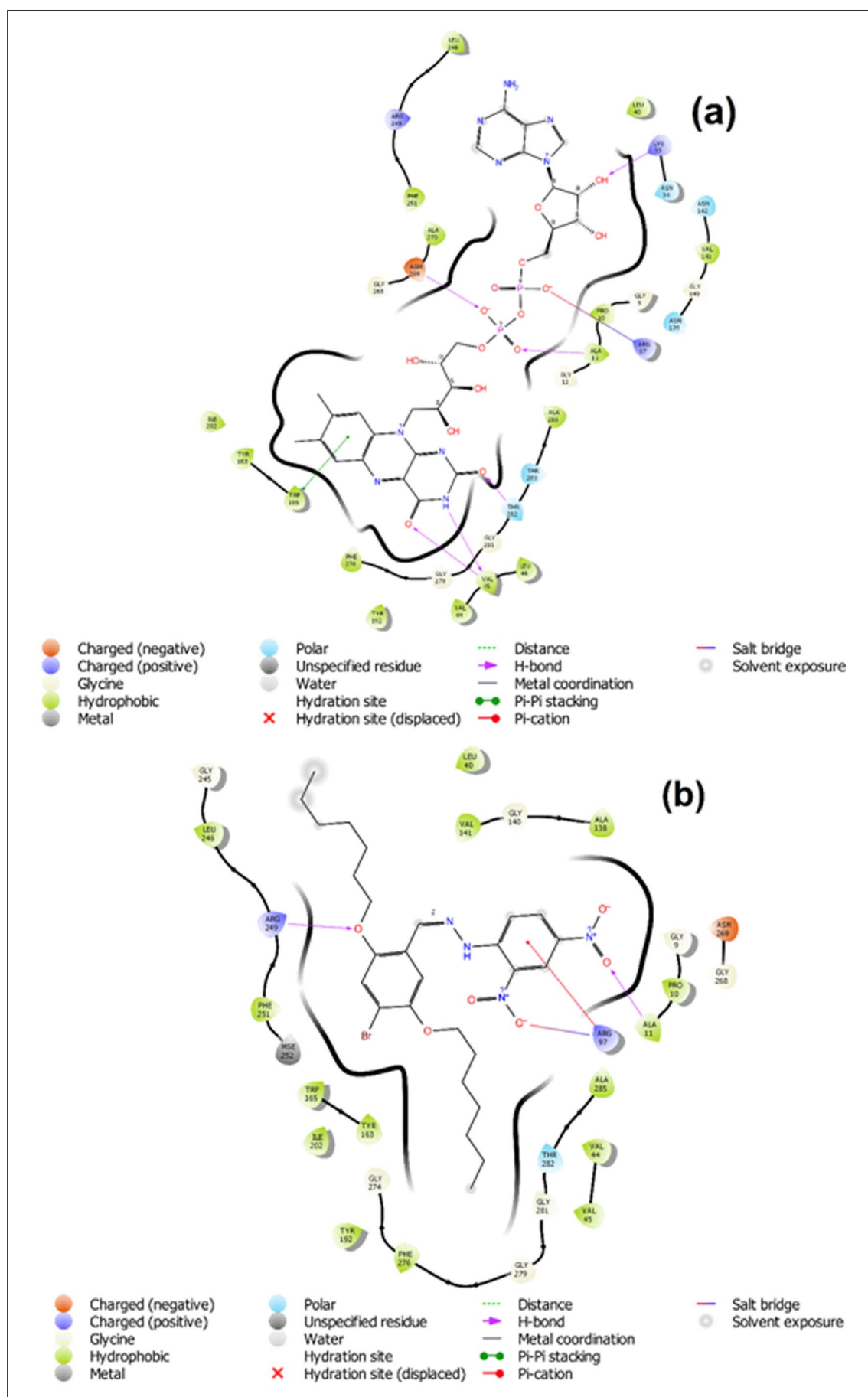


**Figure 2.** A schematic 2D interaction diagram representing the ligand complexes with the *C. violaceum* ATCC 12472-protein receptor (hydrogen bond, salt bridge, hydrophobic interactions): (a) the complex with FAD and (b) the complex with BHBANA (6).



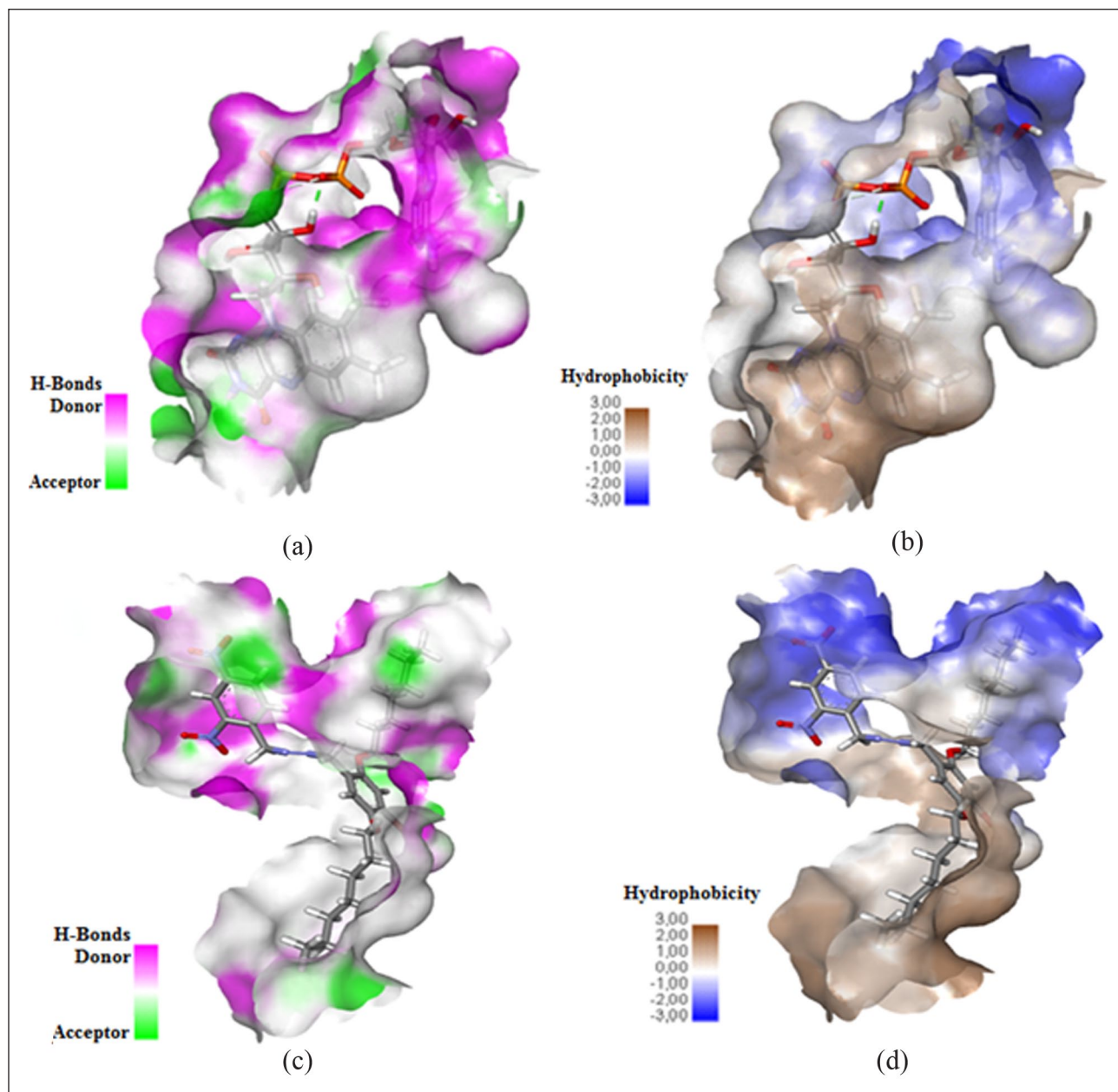


**Figure 3.** 3D orientation of synthetic molecules: (a and c) the hydrogen bonds of the FAD and BHBANA (**6**) molecules and (b and d) the hydrophobic surfaces of FAD and BHBANA (**6**) molecules.

microbial virulence factors through antimicrobial, anti-biofilm, violacein inhibition, anti-quorum sensing, and swarming motility inhibitions. Compound **6** shows promising inhibition of quorum sensing-mediated violacein production in *Chromobacterium* as well as a concentration-dependent inhibition of swarming motility in flagellated *P. aeruginosa* PA01. The molecular interaction analysis established the first foundations for understanding the correlation between structure and anti-quorum sensing activity in this family of compounds that constitutes a basis for further structural modifications. Nevertheless, the obtained outcomes demonstrated that the elaborated modeling evaluation identified BHBANA as an effective inhibitor of the QS system and could lead to inhibition of resistant biofilms. This compound equally inhibited biofilm formation in selected pathogenic microbes at MIC and sub-MIC concentrations.

## Experimental

### Materials

For the synthesis, the reagents and solvents were obtained from Sigma-Aldrich or Fluka and were used without further purification. Thin layer chromatography (TLC) was performed on Merck 60 F<sub>254</sub> silica gel plates. Luria-Bertani broth, nutrient broth, Mueller-Hinton broth, agar-agar, D-(+)-glucose, crystal violet, ethanol, and glacial acetic acid were all obtained from Merck and 96-well microplate reader plates (Greiner Bio-One, sterile, PS, flat-bottom) were used in anti-biofilm tests. Tryptone (Sigma-Aldrich), sodium chloride (Sigma-Aldrich), kanamycin sulfate (Sigma-Aldrich), *N*-hexanoyl-DL-homoserine lactone (C<sub>6</sub>-HSL, ≥97%, Sigma-Aldrich), *N*-decanoyl-DL-homoserine lactone (C<sub>10</sub>-HSL, ≥97%, Sigma-Aldrich), and D-(+)-glucose

**Table 3.** Distances, categories, and types of hydrogen bonding for BHBANA and FAD toward the active sites of CviR.

Amino acid	Distance (Å)		Category		Type	
	BHBANA	FAD	BHBANA	FAD	BHBANA	FAD
GLY140	2.71336	2.75944	H-bond	H-bond	C–H bond	C–H bond
THR282	2.56889	2.87309	H-bond	H-bond	C–H bond	C–H bond
ARG97	2.80087	2.86170	H-bond	H-bond	Pi-donor H-bond	Conventional H-bond
TRP165	5.16286	5.18892	Hydrophobic interaction	H-bond	Pi–Pi stacked	Pi–Pi stacked
TRP165	3.76370	3.96546	Hydrophobic interaction	Hydrophobic interaction	Hydrophobic interaction	Pi–Pi stacked
VAL44	5.37175	–	Hydrophobic interaction	–	Alkyl	–
TYR163	4.92416	4.96877	Hydrophobic interaction	Hydrophobic interaction	Pi–Alkyl	Pi–Alkyl
TYR163	5.36608	5.18187	Hydrophobic interaction	Hydrophobic interaction	Pi–Alkyl	Pi–Alkyl
TRP165	4.32797	3.96546	Hydrophobic interaction	Hydrophobic interaction	Pi–Alkyl	Pi–Pi stacked
PHE276	3.71384	4.30690	Hydrophobic interaction	Hydrophobic interaction	Pi–Alkyl	Pi–Alkyl

BHBANA: *N*-[(*E*)-4-bromo-2,5-diheptyloxybenzylideneamino]-2,4-dinitroaniline.

(≥99.5%, Sigma-Aldrich) were used in anti-QS assays. The MIC was determined using 96-well microplate reader plates (Greiner Bio-One, sterile, PP, U-bottom).

### Instrumentation

The melting points were determined on a Kofler-type apparatus. <sup>1</sup>H and <sup>13</sup>C NMR spectra were recorded in CDCl<sub>3</sub> on a Gemini 300 MHz NMR spectrometer for **3** and **4** and on a Bruker AV300III spectrometer in DMSO-*d*<sub>6</sub> + acetone-*d*<sub>6</sub> 2:1 for (**6**). Infrared spectroscopy (IR) was recorded on a Perkin-Elmer 200 spectrophotometer using KBr. For *N*-[(*E*)-4-bromo-2,5-diheptyloxybenzylideneamino]-2,4-dinitroaniline (BHBANA), high-resolution mass spectrometry (HRMS) was performed on a Maxis 4G instrument at the CRMPO (University of Rennes, France), and 2D NMR (COZY, HMBC, HMQC, NOESY) was performed on a Bruker AV300III spectrometer. A multi-scan Go microplate reader (Thermo Fischer Scientific, Waltham, MA, USA) was used to read optical densities during the MIC tests, biofilm assays, and violacein inhibition studies.

### Synthesis and characterization

**Synthesis of 1,4-dibromo-2,5-diheptyloxybenzene (3).** KOH (48 g, 856 mmol) in anhydrous DMSO (300 mL) was stirred under nitrogen for 2 h at room temperature and 2,5-dibromohydroquinone **2** (24.32 g, 90.80 mmol) followed by 1-bromoheptane (29.96 mL, 190.68 mmol) were then added.<sup>38,65,66</sup> After 3 h, the reaction mixture was added to ice-cold distilled water (300 mL) and a white precipitate was formed. The precipitate was filtered, dried, and recrystallized using acetone/toluene (1:1) to give compound **3** (32.67 g, 78%) as transparent white crystals, m.p. 58.7 °C.

<sup>1</sup>H NMR (300 MHz, CDCl<sub>3</sub>): δ 0.89 (t, 6H, 2 CH<sub>3</sub>, *J*=7.0 Hz), 1.22–1.41 (m, 16H, 2(CH<sub>2</sub>)<sub>4</sub>), 1.80 (q, 4H, 2CH<sub>2</sub>, *J*=6.0 Hz), 3.94 (t, 4H, 2CH<sub>2</sub>O, *J*=7.0 Hz), 7.08 (s, 2H, ArH).

<sup>13</sup>C NMR (75 MHz, CDCl<sub>3</sub>): δ 14.13 (2CH<sub>3</sub>), 22.63 (2CH<sub>2</sub>), 25.93 (2CH<sub>2</sub>), 29.01 (2CH<sub>2</sub>), 29.15 (2CH<sub>2</sub>), 31.79 (2CH<sub>2</sub>), 70.32 (2CH<sub>2</sub>O), 111.13 (2C<sub>quat</sub>, 2C ArBr), 118.46 (2CH, Ar), 150.09 (2C<sub>quat</sub>, 2C Ar).

**Synthesis of 4-bromo-2,5-diheptyloxybenzaldehyde (4).** 1,4-dibromo-2,5-diheptyloxybenzene **3** (8.82 g, 18.99 mmol) was added to diethyl ether (300 mL) and stirred at –10 °C under nitrogen for 30 min. A solution of *n*-butyllithium (1.88 mL, 20.90 mmol, 2.7 M in heptane) was added to the reaction mixture followed by dimethylformamide (DMF) (1.92 mL, 24.92 mmol). The resulting mixture was allowed to react at 15 °C for 2 h while being monitored by TLC. One hundred milliliters of acidified water (10% HCl) was added, and the organic phase was separated and washed with NaHCO<sub>3</sub> solution, dried over CaCl<sub>2</sub>, and evaporated. The product was purified by column chromatography on silica gel with a toluene/hexane mixture (2:1) to afford 6 g of the compound **4** (76% yield, m.p. 59 °C) as pale yellow crystals.<sup>67</sup>

<sup>1</sup>H NMR (300 MHz, CDCl<sub>3</sub>): δ 0.80–0.99 (m, 6H, 2CH<sub>3</sub>), 1.21–1.61 (m, 16H, 2(CH<sub>2</sub>)<sub>4</sub>), 1.76 (q, 4H, 2CH<sub>2</sub>, *J*=6.0 Hz), 3.91 (t, 4H, 2CH<sub>2</sub>O, *J*=7.0 Hz), 7.23 (s, 1H, ArH), 7.31 (s, 1H, ArH), 10.42 (s, 1H, CHO).

<sup>13</sup>C NMR (75 MHz, CDCl<sub>3</sub>): δ 14.07 (2CH<sub>3</sub>), 23.01 (2CH<sub>2</sub>), 23.97 (2CH<sub>2</sub>), 29.05 (2CH<sub>2</sub>), 30.59 (2CH<sub>2</sub>), 39.46 (2CH<sub>2</sub>), 72.11 (2CH<sub>2</sub>O), 110.31 (1CH, Ar), 118.32 (1CH, Ar), 121.08 (1C<sub>quat</sub>, 1C ArBr), 124.26 (1C<sub>quat</sub>, 1C ArCHO), 150.03 (1C<sub>quat</sub>, 1C Ar-O), 155.93 (1C<sub>quat</sub>, 1C Ar-O), 188.87 (1CH, CHO).

Synthesis of *N*-[(*E*)-4-bromo-2,5-diheptyloxybenzylideneamino]-2,4-dinitroaniline (BHBANA) (**6**). 4-bromo-2,5-diheptyloxybenzaldehyde **4** (5 g, 12.09 mmol) was added to a stirred solution of 2,4-dinitrophenylhydrazine (2.5 g, 12.62 mmol) in acidified methanol (20 mL), and the mixture was refluxed at 80 °C for 5 h. The hydrazone product precipitated as an orange solid (87% yield), which was washed with ethanol and dried (m.p. 179 °C).

IR  $\nu_{\max}$  (KBr): 579, 1038, 1210, 1326, 1467, 1501, 1590, 1611, 2851, 2940, 3092, 3289  $\text{cm}^{-1}$ .

HRMS (ASAP source at 160 °C)  $m/z$  [M + H]<sup>+</sup> calcd for C<sub>27</sub>H<sub>38</sub><sup>79</sup>BrN<sub>4</sub>O<sub>6</sub> 593.19692; found: 593.1970,  $m/z$  [M]<sup>+</sup> calcd for C<sub>27</sub>H<sub>37</sub><sup>79</sup>BrN<sub>4</sub>O<sub>6</sub> 592.18910; found: 592.1887,  $m/z$  [M—C<sub>7</sub>H<sub>14</sub> + H]<sup>+</sup> calcd for C<sub>20</sub>H<sub>24</sub><sup>79</sup>BrN<sub>4</sub>O<sub>6</sub> 495.08737; found: 495.0864.

<sup>1</sup>H NMR (300 MHz, DMSO-*d*<sub>6</sub> + acetone-*d*<sub>6</sub>; 2:1):  $\delta$  0.88 (t, 3H, *J*=6.8 Hz, CH<sub>3</sub>), 0.89 (t, 3H, *J*=6.8 Hz, CH<sub>3</sub>), 1.23-1.60 (m, 16H, 8CH<sub>2</sub>), 1.73-1.86 (m, 4H, 2CH<sub>2</sub>CH<sub>2</sub>O), 4.06 (t, 2H, CH<sub>2</sub>O, *J*=6.6 Hz), 4.11 (t, 2H, CH<sub>2</sub>O, *J*=6.2 Hz), 7.36 (s, 1H, ArH), 7.59 (s, 1H, ArH), 8.14 (d, 1H, ArH(DNP), *J*=9.6 Hz), 8.35 (dd, 1H, ArH(DNP), *J*=9.6, 2.7 Hz), 8.89 (d, 1H, ArH(DNP), *J*=2.7 Hz), 8.90 (s, 1H, HC=N), 11.76 (1H, br.s, NH).

<sup>13</sup>C NMR (75 MHz, DMSO-*d*<sub>6</sub> + acetone-*d*<sub>6</sub>; 2:1):  $\delta$  14.05 (2CH<sub>3</sub>), 22.46 (CH<sub>2</sub>), 22.49 (CH<sub>2</sub>), 25.80 (CH<sub>2</sub>), 25.95 (CH<sub>2</sub>), 28.88 (CH<sub>2</sub>), 28.89 (CH<sub>2</sub>), 29.14 (CH<sub>2</sub>), 29.16 (CH<sub>2</sub>), 31.69 (CH<sub>2</sub>), 31.71 (CH<sub>2</sub>), 69.70 (CH<sub>2</sub>O), 69.75 (CH<sub>2</sub>O), 110.20 (CH, Ar), 115.36 (C<sub>quat</sub>, Ar), 117.36 (CH, Ar), 118.63 (CH, Ar), 122.88 (C<sub>quat</sub>, Ar), 123.18 (CH, Ar), 129.77 (CH, Ar), 130.08 (C<sub>quat</sub>, Ar), 137.53 (C<sub>quat</sub>, Ar), 144.30 (CH=N), 144.85 (C<sub>quat</sub>, Ar), 149.77 (C<sub>quat</sub>, Ar), 152.45 (C<sub>quat</sub>, Ar).

### Microbial strains

Two Gram-positive strains, *Staphylococcus aureus* ATCC 25923 and *Enterococcus faecalis* ATCC 29212; two Gram-negative strains, *Escherichia coli* ATCC 25922 and *Pseudomonas aeruginosa* ATCC 27853; and two yeasts, *Candida albicans* ATCC 10239 and *Candida tropicalis* ATCC 13803, were used in the antimicrobial and antibiofilm assays. *Chromobacterium violaceum* CV12472 and *Chromobacterium violaceum* CV026 were used in violacein inhibition and quorum sensing inhibition, respectively. The flagellated strain *Pseudomonas aeruginosa* PA01 was used in the evaluation of motility inhibition in the swarming assay.

### Determination of antimicrobial activity

MIC values of BHBANA (**6**) were evaluated using 96-well microplates by the broth dilution method described elsewhere.<sup>68</sup> The MIC was the lowest concentration of the test compound in which there was no visible microbial growth. Mueller-Hinton broth was used as the medium, and  $5 \times 10^5$  colony-forming units (CFU) mL<sup>-1</sup> of bacterial density was used. Microbial cell suspension (10 mL) was introduced into the wells of the 96-well plate together with the test compound at final concentrations of 5.0, 2.5, 1.25, 0.625, 0.312, and 0.156 mg mL<sup>-1</sup>. The microplates were then

incubated at 37 °C overnight, and the MIC values were deduced based on optical densities.

### Assays of the anti-biofilm activity of the test compounds

The anti-biofilm effect of BHBANA (**6**) at MIC and sub-MIC concentrations (1, 1/2, 1/4, and 1/8 MIC) on test pathogens was evaluated using a microplate biofilm method.<sup>69</sup> One percent of overnight bacterial cultures was introduced into 200  $\mu$ L of Tryptose-Soy broth (TSB) containing glucose (0.25%) with or without the test compound and incubated at 37 °C for 48 h. The wells of the plates were then carefully emptied and rinsed with distilled water to remove the planktonic microbial cells. The control wells contained only broth and bacterial cells. The bacterial cells within the established biofilms were subsequently stained at room temperature by introducing a solution of crystal violet (0.1%) for about 10 min, after which the crystal violet solution was pipetted out. The wells of the plates were then filled with 200  $\mu$ L of either ethanol (70%) or glacial acetic acid (33%) and then shaken gently. The optical densities (ODs) were then recorded at 550 nm using a Thermo Scientific Multiskan FC, Vantaa, Finland spectrophotometer. The anti-biofilm activity expressed as a percentage inhibition of the test compounds was deduced using the formula

$$\text{Biofilm inhibition(\%)} = \frac{OD550_{\text{Control}} - OD550_{\text{Sample}}}{OD550_{\text{Control}}} \times 100$$

### Bioassay for quorum sensing inhibition (QSI) on *C. violaceum* CV026

The quorum sensing inhibition of BHBANA (**6**) was assayed as described elsewhere with slight modifications.<sup>70</sup> Overnight fresh cultures of CV026 (100  $\mu$ L) were mixed with warmly prepared molten soft agar (5 mL) prepared by mixing in deionized H<sub>2</sub>O (200 mL), NaCl (1.0 g), agar (1.3 g), and tryptone (2.0 g), followed by the addition of exogenous acyl-homoserine lactone (20  $\mu$ L) (C<sub>6</sub>HSL, 100  $\mu$ g mL<sup>-1</sup>). The molten agar mixture containing the CV026 bacterial cells was poured gently as an overlay onto the surface of solidified Luria-Bertani agar (LBA) plates. Five-millimeter-diameter wells were made on the plates after solidification and subsequently filled with 50  $\mu$ L of sterilized MIC and sub-MIC concentrations of the test compound. The plates were incubated at 35 °C for 3 days, after which they were observed for anti-QS activity. Formation of a cream-colored circle formed around the well on the purple surface of actively growing CV026 bacteria indicated QSI, and the diameters were recorded and are given in millimeters. For each sample, three parallel assays were conducted, and the QSI value is the average of the inhibition zones.

### Evaluation of violacein inhibition in *C. violaceum* CV12472

The test compound BHBANA was evaluated for its ability to inhibit the synthesis of violacein by *C. violaceum*

ATCC 12472 in a qualitative assay as described previously.<sup>29,71</sup> Overnight fresh cultures of CV12472 (10  $\mu$ L) (0.4 OD at 600 nm) were mixed with LB broth (170  $\mu$ L) in sterilized microplates and the test compounds (20  $\mu$ L) at MIC and sub-MIC concentrations was added. An assay in which the compound was not added (LB broth and CV12472) served as a positive control. The test plates were incubated for 24 h at 35 °C, after which the absorbance was read at 585 nm to determine any reduction of violacein pigment in the control. Violacein inhibition expressed as the percentage inhibition was deduced from the formula

$$\text{Violacein inhibition (\%)} = \frac{\text{OD}_{585\text{control}} - \text{OD}_{585\text{sample}}}{\text{OD}_{585\text{control}}} \times 100$$

### Inhibition of swarming motility on *P. aeruginosa* PA01

The determination of swarming movement in *P. aeruginosa* PA01 was performed according to the literature method.<sup>72</sup> Thus, plates consisting of swarming agar (0.5% agar, 0.5% NaCl, 0.5% D-glucose, and 1% peptone) and MIC, MIC/2, and MIC/4 concentrations of BHBANA (**6**) before solidification were used. Five microliters of *P. aeruginosa* PA01 overnight fresh cultures was point-inoculated on the center of each plate, and plates without compounds were used as controls. Each plate was incubated at 37 °C, and after 24 h, swarming migration was determined by measuring the swarming front diameters and the percentage reduction in swarming calculated for the control plates.

### Molecular docking studies and visualization

To explore the interaction between the targeted *Chromobacterium violaceum* ATCC 12472 and the newly synthesized BHBANA, molecular docking analysis was performed and compared with that of FAD [(2R,3S,4R,5R)-5-(6-aminopurin-9-yl)-3,4-dihydroxyoxolan-2-yl] methoxyhydroxyphosphoryl], used as a reference ligand. All calculations were carried out using Discovery Studio Visualizer (version 2021) software. The X-ray crystal structures of the vioD hydroxylase in complex with FAD from *Chromobacterium violaceum* (Northeast Structural Genomics Consortium Target CvR158) receptor protein were downloaded from the protein data bank (PDB) with the ID code of (PDB: 3C4A).<sup>52,73</sup> The preparation of the protein 3D structure, its reconstruction, and development (addition of missing residues, and removal of water molecules around the receptor) were made with Maestro using the protein preparation wizard, and the 3D structures of BHBANA (**6**), FAD, and CvR158 were retrieved with ligand preparation using the builder panel in Maestro 11.8.<sup>74</sup> For this study, the optimization parameters were a pH of 7.0, in addition to assigned partial atomic charges and potential ionization states. The base OPLS3e force field was employed to optimize and generate the low-energy conformer of the ligand.<sup>75</sup>

### Acknowledgements

The authors gratefully acknowledge Echahid Cheikh Larbi Tebessi University (Tebessa, Algeria), Larbi Ben M'Hidi University (Oum El Bouaghi, Algeria), Mugla Sitki Kocman University (Mugla, Turkey), and Johannes Kepler University (Linz, Austria), for supplying facilities to realize this investigation. Material, administrative, and technical support from the University of Ngaoundere, Cameroon; Mugla Sitki Kocman University, Turkey; and the Dunarea de Jos University, Romania are gratefully acknowledged.

### Declaration of conflicting interests

The author(s) declared no potential conflicts of interest with respect to the research, authorship, and/or publication of this article.

### Funding

The author(s) received no financial support for the research, authorship, and/or publication of this article.

### ORCID iD

Alfred Ngege Tamfu  <https://orcid.org/0000-0001-6683-3337>

### Supplemental material

Supplemental material for this article is available online.

### References

- Landstrom EB, Akporji N, Lee NR, et al. *Org Lett* 2020; 22: 6543–6546.
- La Regina G, Sarkar T, Bai R, et al. *J Med Chem* 2009; 52: 7512–7527.
- Mobinikhaledi A, Jabbarpour M and Hamta A. *J Chil Chem Soc* 2011; 56: 812–814.
- Rollas S and Güniz Küçükgülmez Ş. *Molecules* 2007; 12: 1910–1939.
- Cheng LX, Tang JJ, Luo H, et al. *Bioorg Med Chem Lett* 2010; 20: 2417–2420.
- Török AS, Bag S, Tulsan R, et al. *Biochem* 2013; 52: 1137–1148.
- Ortiz S, Nelson R, Kesternich V, et al. *M. J Chil Chem Soc* 2016; 61: 3081–3084.
- Popiołek Ł. *Int J Mol Sci* 2021; 22: 9389.
- Amine K and Boulebd H. *Mol Divers* 2021; 25: 279–290.
- Akova M. *Virulence* 2016; 7: 252–266.
- Tamfu AN, Boukhedena W, Boudiba S, et al. *Pharmacia* 2023; 69: 973–980.
- Ngege TA, Ceylan O, Fru G, et al. *Y. Res J Biotechnol* 2021; 16: 68–76.
- Aljeldah MM. *Antibiotics* 2022; 11: 1082.
- Tamfu AN, Munvera AM, Botezatu AVD, et al. *Results Chem* 2022; 4: 100322.
- Antimicrobial Resistance Collaborators. *Lancet* 2022; 399: 629–655.
- Sharma D, Misba L and Khan AU. *Antimicrob Resist Infect Control* 2019; 8: 1–10.
- Arab Y, Sahin B, Ceylan O, et al. *Biodiversitas* 2022; 23: 3498–3506.
- Alain KY, Tamfu AN, Kucukaydin S, et al. *LWT* 2022; 12: 114162.
- Costerton JW, Stewart PS and Greenberg EP. *Science* 1999; 284: 1318–1322.
- Hall-Stoodley L and Stoodley P. *Cellular Microbiol* 2009; 11: 1034–1043.

21. Hall-Stoodley L, Costerton JW and Stoodley P. *Nat Rev Microbiol* 2004; 2: 95–108.
22. Vestby LK, Grønseth T, Simm R, et al. *Antibiotics* 2020; 9: 59.
23. Tamfu AN, Ceylan O, Kucukaydin S, et al. *Foods* 2020; 9: 1768.
24. Richards JJ and Melander C. *Chembiochem* 2009; 10: 2287–2294.
25. Tamfu AN, Ceylan O, Kucukaydin S, et al. *LWT* 2020; 133: 110150.
26. Olson ME, Ceri H, Morck DW, et al. *Can J Vet Res* 2002; 66: 86.
27. Ceri H, Olson ME and Turner RJ. *Expert Opin Pharmacother* 2010; 11: 1233–1237.
28. Heidari R, Farajzadeh Sheikh A, Hashemzadeh M, et al. *Mol Biol Rep* 2022; 49: 3811–3822.
29. Landini P, Antoniani D, Burgess JG, et al. *Appl Microbiol Biotechnol* 2010; 86: 813–823.
30. Yang L, Liu Y, Wu H, et al. *FEMS Immunol Med Microbiol* 2012; 65: 146–157.
31. Alfred Ngege T, Kucukaydin S, Ceylan O, et al. *Nat Prod Commun* 2021; 16: 1–8.
32. Tamfu AN, Ceylan O, Fru GC, et al. *Microbial Path* 2020; 144: 104191.
33. Ceylan O, Tamfu AN, Doğaç Yİ, et al. *3 Biotech* 2020; 10: 513.
34. Kocak G, Tamfu AN, Bütün V, et al. *J Appl Polym Sci* 2021; 138: 50466.
35. Boudiba S, Tamfu AN, Berka B, et al. *Nat Prod Commun* 2021; 16: 1–11.
36. Wang W, Li D, Huang X, et al. *Molecules* 2019; 24: 3792.
37. O'Reilly MC, Dong SH, Rossi FM, et al. *Cell Chem Biol* 2018; 25: 1128–1139.
38. Boudiba S, Adam G, Ulbricht C, et al. *EDP Sciences* 2022; 354: 03003.
39. Khamaysa OMA, Selatnia I, Zeghache H, et al. *J Mol Liq* 2020; 315: 113805.
40. Khamaysa OMA, Selatnia I, Lgaz H, et al. *Colloids Surf* 2021; 626: 127047.
41. Saouli S, Selatnia I, Zouchoune B, et al. *J Mol Struct* 2020; 1213: 128203.
42. Dammene Debbih O, Sid A, Bouchene R, et al. *Acta Crystallogr, Sect C: Struct Chem* 2018; 74: 703–714.
43. Dogancı MA, Sal FA, Guler HI, et al. *World J Microbiol Biotechnol* 2022; 38: 1–14.
44. Alfred TN, Ceylan O, Kucukaydin S, et al. *Bull Environ Pharmacol Life Sci* 2020; 9: 132–142.
45. Pantanella F, Berlutti F, Passariello C, et al. *J Appl Microbiol* 2007; 102: 992–999.
46. Choi SY, Yoon KH, Lee JI, et al. *Biomed Res Int* 2015; 2015: 465056.
47. Kothari V, Sharma S and Padia D. *Asian Pac J Trop Med* 2017; 10: 744–752.
48. Escobar-Muciño E, Arenas-Hernández MMP and Luna-Guevara ML. *Microorganisms* 2022; 10: 884.
49. Tamfu AN, Ceylan O, Cârâc G, et al. *Molecules* 2022; 27: 4872.
50. Beddiar H, Boudiba S, Benahmed M, et al. *Plants* 2021; 10: 1955.
51. Lamin A, Kaksonen AH, Cole IS, et al. *Bioelectrochemistry* 2022; 145: 108050.
52. Amaning Danquah C, Minkah PAB, Osei Duah Junior I, et al. *Antibiotics* 2022; 11: 285.
53. Leisner JL. *Front Microbiol* 2020; 11: 976.
54. Nadar S, Khan T, Patching SG, et al. *Microorganisms* 2022; 10: 303.
55. Tamfu AN, Kocak G, Ceylan O, et al. *J Appl Polym Sci* 2023; 140: e53631.
56. Francolini I and Donelli G. *FEMS Immunol Med Microbiol* 2010; 59: 227–238.
57. Khatoun Z, McTiernan CD, Suuronen EJ, et al. *Heliyon* 2018; 4: e01067.
58. Oura H, Tashiro Y, Toyofuku M, et al. *Appl Environ Microbiol* 2015; 81: 2808–2818.
59. Tamfu AN, Kucukaydin S, Ceylan O, et al. *Chem Africa* 2021; 4: 759–767.
60. Hou L, Debru A, Chen Q, et al. *Front Microbiol* 2019; 10: 1847.
61. Lakshmanan A, Harikrishnan A, Vishnupriya S, et al. *ACS Omega* 2019; 4: 16994–16998.
62. Tamfu AN, Kucukaydin S, Quradha MM, et al. *Chem Africa* 2022; 5: 237–249.
63. Ran T, Gao M, Wei Q, et al. *Acta Crystallographica Section F: Struct Biol Com* 2015; 71: 149–152.
64. Venkatramanan M, Sankar Ganesh P, Senthil R, et al. *ACS Omega* 2020; 5: 25605–25616.
65. Boudiba S, Růžička A, Ulbricht C, et al. *J Polym Sci Part A: Polym Chem* 2017; 55: 129–143.
66. Moy CL, Kaliappan R and McNeil AJ. *J Org Chem* 2011; 76: 8501–8507.
67. Egbe DAM, Roll CP, Birckner E, et al. *Macromolecules* 2002; 35: 3825–3837.
68. Merritt JH, Kadouri DE and O'Toole GA. *Curr Protoc Microbiol* 2005; 1: 853.
69. Ikome HN, Tamfu AN, Abdou JP, et al. *Appl Biochem Biotechnol*. Epub ahead of print 22 February 2023. DOI: 10.1007/s12010-023-04380-6.
70. Koh H and Tham FY. *J Microbiol Immunol Infect* 2011; 44: 144–148.
71. Popova M, Gerginova D, Trusheva B, et al. *Foods* 2021; 10: 997.
72. Packiavathy ASVP, Agilandeswari, Musthafa KS, et al. *Food Res Int* 2012; 45: 85–92.
73. Durán N, Justo GZ, Durán M, et al. *Biotechnol Adv* 2016; 34: 1030–1045.
74. Roos K, Wu C, Damm W, Reboul M, et al. *J Chem Theory Comput* 2019; 15: 1863–1874.
75. Lig Prep. Schrödinger Release 2021-4. S, LLC. New York: Schrödinger, 2021.